Charge Qubits in Doped Quantum Dots : Effects on Computation and Coherence

[1*] Thierry Ferrus, [1]Tsung-Yeh Yang, [2]Yu Yamaoka, [2]Tomohiro Kambara, [2]Tetsuo Kodera, [2]Shunri Oda and [1]David Arfon Williams
[1]Hitachi Cambridge Laboratory, J J Thomson avenue, CB3 0HE, Cambridge, United Kingdom
[2]Department of Physical Electronics, Quantum Nanoelectronics Research Centre, Tokyo Institute of Technology, Tokyo, 152-8552 Japan
* Email: taf25@cam.ac.uk

***Abstract*—Doping in quantum information architectures is often presented as a source of decoherence for the qubit to study. However, high doped material also present additional properties that could be used in quantum computation. Here, we show that the application of GHz photons to a doped double quantum dot allows a pair of active dopant to be selected and gate operation to be implemented with potential coherence time exceeding 200 μs.**

***Index Terms*—Quantum computing; silicon; charge qubit; quantum dots**

I. INTRODUCTION

In a previous paper, we did present a scalable and industrially compatible architecture for performing quantum computation [1]. In this proposal, qubit states are defined by the spatial location of an extra charge in an highly doped double quantum dot (IDQD) [2][3]. The structure is realized by implanting at high dose phosphorous atoms into the 40-nm thick silicon layer of a silicon-on-insulator (SOI) wafer to obtain an effective doping density of about 3 10^{19} cm^{-3}. Full electrical insulation of the qubit is then achieved by etching away any conducting material between the various structures (gates, detector and qubit), a method leading to a significant decrease in the electron temperature of the qubit [4]. The device is further encapsulated by a 12-nm thick thermal silicon oxide with a final value for the dot diameter reaching about 60 nm. Doping by phosphorous atoms and the realization of constrictions in order to define the quantum dot tunnel barriers offer a substitutionary method to standard Metal-Oxide-Semiconductor (MOS) device fabrication, enhancing the scalability possibilities.

Despite attractiveness for manufacturing purposes, doped architectures are rarely used in practical qubit implementations and, most of the research on charge or spin qubits concentrates on the use of fin field effect transistors (FinFETs) or nanoscale transistor technology pushing the well know Moore law [5] below the 100-nm scale [6]. One obvious justification is the presence of dopants that are often associated with localization effects, especially at interfaces, causing random telegraph signal events and contributing to electronic noise. Ensemble of donors may also be difficult to manipulate due to electron-electron interaction and glassy behavior that may arise near the metal-to-insulator transition [7], whereas controlling single donors has not been possible until recently [8].

In this paper, we would like to discuss some major differences in operation between doped and undoped qubits, showing in particular that dopants are not necessarily detrimental to qubit operations if an adapted control is designed. We also discuss some surprising striking consequences on the value of coherence time in doped quantum dots and give some insight for the realizing spin qubits in a doped environment.

In Section II, we first discuss the realization charge qubit states in semiconductors. We then describe the differences in pulsing experiments between a doped (Sec. III. A.) and undoped device (Sec. III. B.), bringing the notion of $dopant\ degeneracy$. Effects on coherence are discussed in Section IV before some conclusions and comments on scalability are drawn.

II. CHARGE QUBIT STATES IN SILICON

Within the large number of qubit implementations, charge qubits are one of the simplest ways to realize quantum computation in semiconductors and, in particular, silicon. There are two possible qubits that could be implemented. In the first case, localized states are used and the $\mid 0\rangle$ and $\mid 1\rangle$ are defined by the spatial location of a charge in a double quantum dot. In this case, the quantum gate $\mid \sigma_x\rangle$ is simply implemented by the tunneling of an electron between the two dots across the tunnel barrier. Another possibility is to use hybridized states so that qubits states are defined by the bonding-antibonding states, similarly to the hydrogen molecule model. In both cases, there is the need for confinement. There are currently two different methods for achieving this.

The first is to use a standard Metal-Oxide-Semiconductor layer in order to create a two-dimensional electron gas at the Si-SiO$_2$ interface (Fig. 1a). A change in the voltage applied to the top metal gate will bend the silicon conduction band, accumulating electrons at the interface. This allows an easy control of the electron density and the single electron regime can potentially be attained in nanoscale structures and a double dot system can be created from corner states [9]. Confinement itself is then attained by shaping the gate around a predefined etched silicon dot or wire and then realizing a FinFET structure or by reducing the gate length to several tens of nanometers. In some structures, an additional back-gate can be used and gives the ability to control independently the electron-electron interaction and the disorder strength [10]. However, these types

Copyright (c) IARIA, 2015. ISBN: 978-1-61208-431-2

of devices are in general very susceptible and sensitive to defects, in particular Pb centers [11] resulting from the lattice mismatch between silicon and silicon oxide. Reliability of quantum operations also relies on a high quality oxide and, in the case of SiO_2, it should be free of fast diffusers like ions (K^+, Na^+...) or heavy metals (Cu, Au, Cr...) as this induces localized states at the interface [12]. This is potentially a problem for quantum computing schemes as this type of traps tend to localize spins 1/2 at the Si-SiO_2 interface.

The other possible method consists in implanting atoms at high dose and at energies exceeding few tens of keV that will substitute themselves to silicon atoms. In the case of phosphorous, the atom is pentavalent whereas silicon atoms have four covalent bonds (Fig. 1b). This leaves an extra free electron in the lattice and, at high concentration, this method provides a sufficiently high electron density so that conduction occurs in the device despite natural silicon being intrinsic and insulating at low temperatures. In this case, quantum dots are defined by etching away parts of the doped material and by realizing two constrictions where tunnel barriers are most likely to be formed due to the local modification of the electrostatic potential (Fig. 1c). It is important to realize that, some localized states will still be present even at very high concentration. This is the results of i) dielectric screening that enhance electron trapping around Pb centers at the Si-SiO_2 interface as well as phosphorous atoms that have diffused into the oxide during the device process, ii) partial electron screening at the center of the dot due to non-uniform doping and long-range disorder due to distant traps. Density of states for these localized centers is in general small but influence greatly transport properties. Here, most of the noise source arises from defects at the edge of the structure where non-(100) surfaces are present. Edge localization could be important and is responsible for the commonly observed aperiodic conductivity background in quantum dot transport measurements [2].

III. PULSING EXPERIMENTS AND THE DOPANT DEGENERACY

To operate a qubit, a set of quantum gates have to be defined so that the Bloch sphere could be entirely accessible and a pulsing scheme have to be devised. The latter is generally implemented by a series of DC voltage pulses applied to one or several gates or a series of microwave pulses at given frequencies and powers. For both methods, there is conceptually a major difference between doped and undoped devices.

A. Undoped devices

In a MOS-based quantum dot, quantum levels are well defined and their energies in the absence of gate or source-drain biases are generally well approximated within the constant interaction model [13]:

$$E = \sum_{i}^{n} n_i \varepsilon_i + n^2 e^2 / 2C \qquad (1)$$

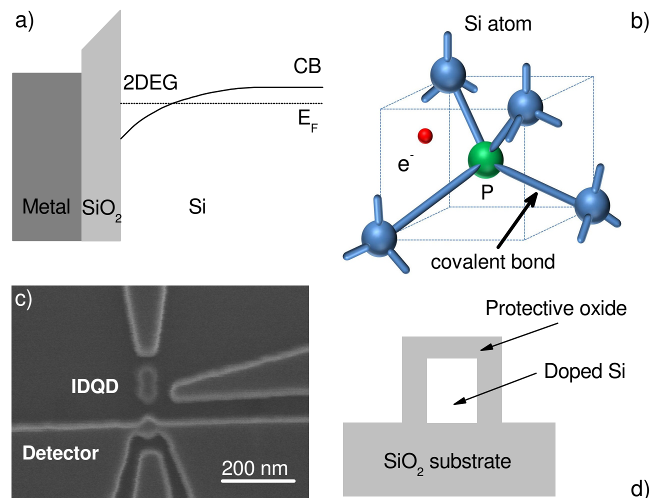

Fig. 1. a) 2D electron gas formation in a MOS structure. b)Structure of the silicon lattice after implantation with phosphorous atoms. c) SEM image showing an IDQD with its charge detector. d) Typical structure of a doped device.

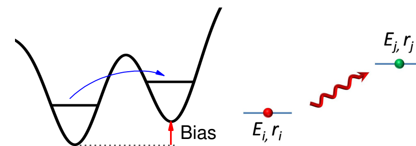

Fig. 2. Photon assisted tunneling in undoped devices.

where ϵ_i and n_i are respectively the single particle state energies due to the quantum dot energy quantization and the occupation number of the level i, n the quantum number and C the capacitance of the quantum dot that is linked to its diameter R by $C = 4\pi\epsilon_0 R$ where $\epsilon_0 \sim 11.7$ is the dielectric constant in silicon.

In the case of a DC pulse, the voltage at the end of the gate modifies the electric potential of the double dot. Quantized energies then acquire an additional term proportional to the pulse amplitude and dependent on the capacitive coupling between the gate and the qubit. This leads to a change in the structure of the levels that modifies the electron tunneling between the two dots (localized states) or modifies the double dot wavefunction (hybridized states).

If photons are to be used for realizing quantum operations, then the relative position of the levels of each dot remains unchanged and gets determined by the predefined values of the gate voltage. Photon assisted tunneling [14] is then used to perform gate operations. The resonant condition is obtained when the photon energy matches the difference in level energies. This effect is much less disturbing for the double dot as levels are not modified during the operation and consequently, this method is less sensitive to the eventual surrounding traps (Fig. 2)

Copyright (c) IARIA, 2015. ISBN: 978-1-61208-431-2

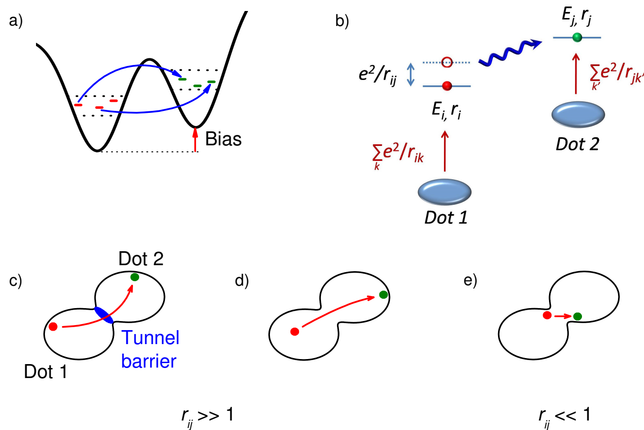

Fig. 3. Photon assisted tunneling in doped devices : a) non-equivalent tunneling, b) Microwave induced tunneling, c)-d) Possible site pairs involved.

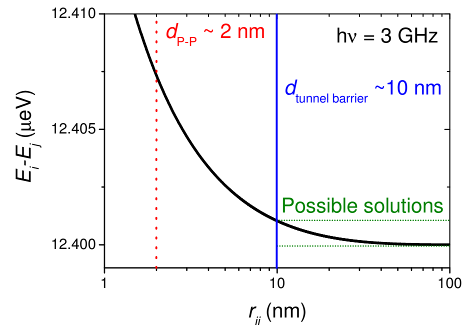

Fig. 4. Solutions of Eq. 2 for a 10 nm tunnel barrier and hν = 3 GHz.

B. Doped devices

In doped devices, the situation is far more complex. The presence of a narrow band of levels and surrounding traps lift the degeneracy that would have prevailed in the absence of disorder. Consequently, not all tunneling events remain equivalent (Fig. 3a). This makes a substantial difference with the undoped version of the device. It is important to notice that degeneracy should be recovered in principle if the temperature exceeds the average level energy spacing within the band but, this is not observed in practice. The reason comes from the bad thermalization of these structures by the phonon bath due to the phonon wavelength getting smaller than the dot dimensions ($\lambda_\gamma \sim 26$ nm in highly doped silicon at 4.2 K [15]). As a result, excitations with energies below $k_B T$ can still be observed if the process involves a timescale shorter than the thermalization time and the longitudinal relaxation time T_1.

One consequence on DC pulsing, is that the pair of sites involved in the tunneling may not be the same if the experiment is repeated under the same conditions despite a single charge being transferred across the tunnel barrier each time. Although semi-classical operations like quantum-cellular-automata could be preformed with high probability, coherence may be affected in the quantum case. However, the situation is much different with photons. Indeed, it has been proposed recently [16] that, in doped devices, microwave photons can both select a pair of sites by their energy difference but also by their spatial location, so that the resonant condition differs sensibly from the usual photon assisted tunneling's by the addition of a interaction term (Fig. 3b):

$$h\nu = E_j - E_i - e^2/(4\pi\epsilon_0 r_{ij}) \exp(-r_{ij}/\lambda_{TF}) \quad (2)$$

$\lambda_{TF} \sim n_e^{-1/2}$ is the Thomas-Fermi screening length and takes into account the presence and influence of the other electrons at a density of n_e. E_i and E_j are the respective level energies of site i and j whereas r_{ij} is the distance between the two sites.

If the two sites are spatially distant, the Coulomb term becomes negligible and resonance frequencies in the GHz range imply a substantial difference in levels energies. This situation can be encountered mostly at the edge of the structure where localized states and disorder are present and so, where the density of states has long tails (Fig. 3c). At the center of the dots, the individual wavefunctions overlap quite significantly leading to an effective screening by other surrounding electrons. Consequently, strong localization seems unlikely. However, the presence of acceptors (for example Boron that is used in p-type silicon wafer as background doping) that are trivalent and can consequently create a vacant site in silicon, can locally affect electron screening and weak localization is possible around such a defect. This would allow electrons to tunnel between two sites at the center of the dot (Fig. 3d). Indeed, recent simulations have shown that, in the case of trap formation at the center of the dot, electron screening is only partial.

On the contrary, if the sites are spatially close then Coulomb interaction is strong and sites involved are most likely located at or near the tunnel barriers (Fig. 3e).

C. Site pair selection and effect on coherence

Microwave pulsing is particularly adapted to doped structures due to its ability to select pairs of sites within a highly doped environment. However, for quantum computation, high fidelity has to be achieved and coherence time should be as long as possible, so the active pair has to be isolated from all the other possible pairs for at least T_1. The apparent difficulty in achieving this comes from the fact that the solution of equation 2 is, a priori, not unique and that the number of possible pairs depends both on the trap distribution and the disorder strength, e.g. the shape of the density of states of the localized states. Figure 4 shows possible solutions of Eq. 2 allowing charge tunneling between the two IDQD dots separated by a 10-nm tunnel barrier in the case hν = 3 GHz. This is in contrast with experimental findings where the uniqueness of the pair and long coherence times have been previously reported [16],[17].

Copyright (c) IARIA, 2015. ISBN: 978-1-61208-431-2

In the case of a double quantum dot, the two high electron density regions are separated by a tunnel barrier and, to realize a σ_x rotation, a pair of sites have to be found on either sides of the tunnel barrier. With the exception of localized states at the edges of the structure or lattice defects, these pairs are mostly non-interacting owing to the large distance between the two sites and screening in the high density regions. However, we can show that single electron tunneling between the two IDQD dots is still possible in the case of weakly localized and screened states. In this case, the situation is indeed very similar to how microwaves can select a resonant pair of Rydberg atoms within a large ensemble and how the population of excited states is limited, in practice [18]. In the present case, microwaves can be used to excite one electron from one site i in one of the dot to a higher level (excited states or virtual states) where Coulomb interaction with the other vacant site j from the other dot is unscreened. This microwave-induced interaction adds the Coulomb term e^2/r_{ij} that was initially screened. The other possible pairs (k, k') now becomes non-resonant allowing many oscillations to occur between the two sites before loss of coherence. This phenomenon is well known as $dipole\ blockade$. At sufficiently short distances, dipole interaction may be non-negligible and additional terms in $1/r_{ij}^3$ may need to be taken into account. Considering that the limiting factor will either be the electron-phonon coupling strength or the timescale for interaction with the surrounding electrons, both being respectively weak and long in this type of device, the coherence time could potentially be as large as $2T_1$. Yet, the experimental value of T_1 is surprisingly large and can exceed several 100 μs [19] due to the glassy behavior of doped materials. Consequently, it is possible to envision that the coherence time T_2 could be as large as 200 μs despite the very high doping concentration. Current experiments are actually ongoing to investigate this possibility.

IV. CONCLUSION

We have shown that doped double quantum dots can offer interesting opportunities for optical manipulation in the microwave range by allowing to address a single pair of donors individually located in each dot of a double quantum dot structure. Surprisingly, the process is coherent with a large coherence time due to microwave-induced blockade for the other possible states. Such a selection process for a pair of sites can thus potentially be extended to the realization of spin qubits in a dopant-rich environment.

ACKNOWLEDGMENT

This work was partly supported by JSPS KAKENHI Grants-in-Aid (Nos. 26709023, 26630151, and 26249048), and the Project for Developing Innovation Systems of the Ministry of Education, Culture, Sports, Science and Technology (MEXT) of Japan.

REFERENCES

[1] T. Ferrus, A. Rossi, A. Andreev, P. Chapman, and D. A. Williams, *Quantum Computing with Charge States in Silicon : Towards a Leadless Approach*, 5th International Conference on Quantum, Nano and Micro Technologies, 2011, pp 41.

[2] T. Ferrus, A. Rossi, M. Tanner, G. Podd, P. Chapman, and D. A. Williams, *Detection of charge motion in a non-metallic silicon isolated double quantum dot*, New J. Phys., vol 13, no 10, 2011, pp 103012.

[3] A. Rossi, T. Ferrus, G. J. Podd, and D. A. Williams, *Charge Detection in Phosphorus-doped Silicon Double Quantum Dots*, Appl. Phys. Lett., vol 97, 2010, pp. 223506.

[4] A. Rossi, T. Ferrus, and D. A. Williams, *Electron temperature in electrically isolated Si double quantum dots*, Appl. Phys. Lett., vol 100, no 13, 2012, pp. 133503.

[5] G. Moore, *Cramming More Components onto Integrated Circuits*, Electronics Magazine, vol. 38, No. 8, 1965

[6] H. Sellier, et al, *Transport Spectroscopy of a Single Dopant in a Gated Silicon Nanowire*, Phys. Rev. Lett., vol 97, 2006, pp 206805; V. Deshpande, et al, *Scaling of Trigate Nanowire (NW) MOSFETs Down to 5 nm Width: 300 K Transition to Single Electron Transistor, Challenges and Opportunities*, Solid-State Device Research Conference (ESSDERC), 2012 Proceedings of the European , 2012, pp.121,124.

[7] S. Bogdanovich and D. Popovic, *Onset of Glassy Dynamics in a Two-Dimensional Electron System in Silicon*, Phys. Rev. Lett., vol 88, 2002, pp 236401.

[8] J. J. Pla, et al, *High-fidelity readout and control of a nuclear spin qubit in silicon*, Nature, vol 496, no 7445, 2013, pp 334-338.

[9] M. F. Gonzalez-Zalba, S. Barraud, A. J. Ferguson and A. C. Betz, *Probing the limits of gate-based charge sensing*, Nature Communications, vol 6, 2015, pp 6084.

[10] A. Lewalle, et al, *Relative importance of the electron interaction strength and disorder in the two-dimensional metallic state*, Phys. Rev. B, vol 66, 2002, pp 075324.

[11] G. J. Gerardi, E. H. Poindexter, P. J. Caplan and N. M. Johnson, *Interface traps and Pb centers in oxidized (100) silicon wafers*, Appl Phys Lett, vol 49, 1986, pp 348-350.

[12] T. Ferrus, R. George, C. H. W. Barnes and M. Pepper, *Disorder and electron interaction control in low-doped silicon metal-oxide-semiconductor field effect transistors*, Appl. Phys. Lett., vol 97, no 14, 2010, pp 142108.

[13] C. W. J. Beenaker, Theory of Coulomb-blockade oscillations in the conductance of a quantum dot, Phys. Rev. B 44, vol 4, 1991, pp 1646-1656. D. V. Averin, A. N. Korotkov, and K. K. Likharev, Theory of single-electron charging of quantum wells and dots, Phys. Rev. B 44, vol 12, 1991, pp 6199-6211. S. Oda and D. Ferry, *Silicon nanoelectronics*, Taylor and Francis, CRC Press, 2006, pp 159-160.

[14] L. P. Kouwenhoven, et al, *Photon-assisted tunneling through a quantum dot*, Phys. Rev. B, vol 50, 1994, pp 2019-2022; G. Platero and R. Aguado, *Photon-assisted transport in semiconductor nanostructures*, Physics Reports, vol 395, 2004, pp 1-157.

[15] J. Seyler and M. N. Wybourne, *Acoustic waveguide modes observed in electrically heated metal wires*, Phys. Rev. Lett., vol 69, 1992, pp 1427-1430.

[16] T. Ferrus, et al, *GHz photon-activated hopping between localized states in a silicon quantum dot*, New J. Phys., vol 16, no 1, 2014, pp 013016.

[17] J. Gorman, D. G. Hasko, and D. A. Williams, *Charge qubit operation of an isolated double quantum dot*, Phys. Rev. Lett., vol 95, 2005, pp 090502.

[18] M. D. Lukin, et al, *Dipole Blockade and Quantum Information Processing in Mesoscopic Atomic Ensembles*, Phys. Rev. Lett., vol 87, 2001, pp 037901; E. Urban, et al, *Observation of Rydberg blockade between two atoms*, Nat. Phys., vol 5, 2009, pp 110; M. Weidemuller, *Rydberg atoms: There can be only one*, Nature Physics 5, 2009, pp 91-92.

[19] T. Ferrus, et al *Cryogenic instrumentation for fast current measurement in a silicon single electron transistor*, J. Appl. Phys., vol 106, 2009, pp. 033705.